Quantum Control of the Angular Momentum Distribution in Multiphoton Absorption Processes

Nirit Dudovich, Dan Oron, and Yaron Silberberg

Department of Physics of Complex Systems, Weizmann Institute of Science, Rehovot 76100, Israel

(Received 7 October 2003; published 12 March 2004)

The newly developed technique of polarization pulse shaping is applied to the control of two-photon absorption in atomic rubidium. This technique enables the manipulation of the *transient vector* properties of a light matter interaction. We establish that control can be exerted on the angular distribution of the final state, and demonstrate the ability to control the final state population of a nearly degenerate system, as well as to perform M-state resolved spectroscopy.

DOI: 10.1103/PhysRevLett.92.103003 PACS numbers: 32.80.Qk, 39.30.+w

The ability to tailor the temporal shape of an ultrashort pulse enables the manipulation of the evolution of a quantum system and thus the control of various atomic and molecular processes. Quantum coherent control is achieved by controlling the interference between different quantum paths that reach the same final state. Several schemes for the control of such interferences have been proposed [1–3] and demonstrated [4–10] for numerous atomic and molecular systems. In particular, control of the spectral phase of the pulse and thus its temporal profile, enabled control over the dynamics of various processes [4–6]. Control over the two-photon absorption (TPA) process, which is the simplest controllable multiphoton process, exemplifies the strength of such techniques. A nonresonant TPA process can be reduced and even eliminated using shaped pulses [7]. Similar techniques can enhance resonant TPA beyond the level achieved by a transform limited pulse [8–10].

However, in all these different coherent control schemes the degree of control is limited. It is impossible to separate between degenerate paths, within the resolution of the pulse shaper. This restriction applies also for intermediate states, so that independently of the number of intermediate states, the different transition moments are reduced, effectively, to a single scalar value. In this Letter we establish that a higher degree of controllability can be achieved by applying vectorial spectral manipulation to the laser pulse.

Phase-and-polarization pulse shaping was recently demonstrated by Brixner *et al.* [11]. In principle, polarization manipulation of the laser field should enable control of the *vector* properties of this interaction. Asaro *et al.* [12] have proposed a polarization control scheme, in which variation of the polarization of a CW laser field enables control of the branching ratio between different photodissociation channels.

When the transition is induced by ultrashort pulses, the *transient vector* properties of the transition can be controlled [13]. In this Letter we present a new coherent control scheme to manipulate multiphoton transitions to degenerate levels by controlling both the spectral phase and spectral polarization of the ultrashort pulse. Using this scheme we achieve independent control of the population of different final states characterized by a different angular momentum change in a TPA transition. Furthermore, we demonstrate control by interfering paths that pass through degenerate intermediate states with different angular momentum.

Consider TPA in an atomic system, induced by a weak femtosecond laser pulse with an electric field $\vec{\varepsilon}(t)$. The amplitude of the excited state at $t \rightarrow \infty$, as predicted by 2nd order time dependent perturbation theory, is given by

$$a_f = \frac{-e^2}{\hbar^2} \sum_n \int_{-\infty}^{\infty} d\omega \frac{\langle f|\vec{E}(\omega_{fg} - \omega)|n\rangle\langle n|\vec{E}(\omega)|g\rangle}{\omega_{ng} - \omega}, \quad (1)$$

where $|g\rangle$, $|n\rangle$, and $|f\rangle$ are the ground, intermediate, and final levels, respectively. Each of the levels is characterized by three quantum numbers $|g, F, M\rangle$, $|n, F', M'\rangle$, and $|f, F'', M''\rangle$, $\omega_{ij} = (E_i - E_j)/\hbar$, $\vec{E}(\omega)$ is the Fourier transform of $\vec{\varepsilon}(t)$ and the summation is performed over all possible intermediate states of the unperturbed atom. The pulse duration is assumed to be considerably shorter than all lifetimes involved.

Equation (1) reflects the fact that two-photon transitions occur for all pairs of photons with frequencies that sum up to the final transition energy [7]. The transition to the different $|f, F'', M''\rangle$ depends on the spectral polarization of the laser field. Specifically, in a two-photon absorption process the angular momentum change of an atom depends on the total momentum of all photon pairs that contribute to a specific final state. Consider a simplified case in which the spectral polarization is composed of only two orthogonal linear polarizations. We choose $\hat{x}$ and $\hat{y}$ to be parallel and perpendicular to the quantization axis, respectively. The population amplitude is given by

$$a_{|f,F,M\rangle} = \frac{-e^2}{\hbar^2}\sum_n \int_{-\infty}^{\infty} [\{\mu^0_{nf}\mu^0_{gn}E_x(\omega)E_x(\omega_{fg}-\omega) + 2\mu^{-1}_{nf}\mu^1_{gn}E_y(\omega)E_y(\omega_{fg}-\omega)\}\delta(\Delta M,0) + \{\mu^{\pm1}_{nf}\mu^0_{gn}E_x(\omega)E_y(\omega_{fg}-\omega) + \mu^0_{nf}\mu^{\pm1}_{gn}E_y(\omega)E_x(\omega_{fg}-\omega)\}\delta(\Delta M,\pm1) + \mu^{\pm1}_{nf}\mu^{\pm1}_{gn}E_y(\omega)E_y(\omega_{fg}-\omega)\delta(\Delta M,\pm2)] \times \frac{1}{\omega_{ng}-\omega}d\omega, \quad (2)$$

where ΔM is the total angular momentum change and $\mu^{\pm1,0}_{ij}$ are the dipole moment matrix elements related to an angular momentum change of the one photon transition.

The population amplitude of a particular state which posseses an angular momentum change ΔM, is determined by the interference of all the photon pairs with frequencies $\omega, (\omega_{fg}-\omega)$ with the respective total momentum, as reflected by the different terms in (2). Each of these terms can be controlled by applying appropriate phases to the optical fields $E_i(\omega)$, as previously shown for two-photon transitions [7,8]. In addition, by employing spectral polarization manipulation, phase control can be applied separately to transition of a specific ΔM. For an M-selected initial state, this directly determines the angular momentum distribution at the final state. For a nonselected initial state, the final yield is an incoherent sum of the transitions from all the different states. The transition from each of these initial M states depends, however, only on ΔM and not on M itself.

To demonstrate angular distribution control, we considered TPA in rubidium gas between the $5S$ and the $5D$ states [Fig. 1(a)]. The TPA was induced by pulses with a bandwidth of 30 nm (corresponding to 30 fs transform limited pulses) centered at the two-photon transition frequency $\omega_{fg}/2$ (778 nm). The TPA rate is evaluated by measuring the fluorescence at ~420 nm due to spontaneous decay to the ground level through the $6P$ level. Spectral phases and polarizations were applied by a programmable pulse shaper, which includes two liquid crystal spatial light modulator (SLM) arrays whose preferential orientation axes are at right angles to each other [11], and are rotated by ±45° relative to the polarization of the input beam. Any difference in the applied retardance between the the two arrays results in modification of the input beam polarization. An additional retardance applied to both arrays modifies the spectral phase. The spectral resolution, determined by the spot size at the Fourier plane, is about 0.3 nm. In order to avoid a spectral overlap with the resonant $5S-5P_{3/2}$, $5S-5P_{1/2}$ transitions (780, 795 nm), spectral parts of the pulse are blocked such that the TPA process is effectively induced by two spectral bands, each 10 nm wide, centered around 769 and 789 nm, and is thus practically nonresonant. The shaped pulse is focused into a Rb cell heated to 80°C with a 5 cm achromatic lens. The fluorescence signal is filtered out and measured with a photomultiplier tube (PMT) and a lock-in amplifier. An outline of the experimental setup is presented in Fig. 1(b).

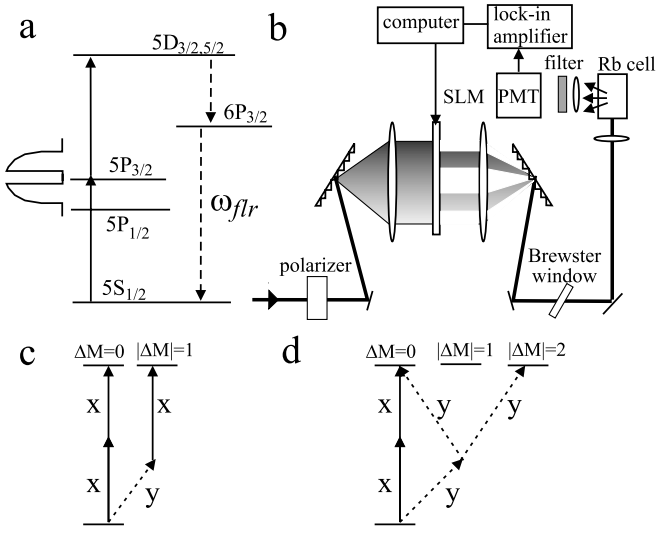

FIG. 1. (a) Energy level diagram of the two photon transition $5S \rightarrow 5D$ in atomic Rb. Wavelengths shorter than 761 nm are blocked as they spectrally overlap the $5S \rightarrow 7S$ transition. (b) Outline of the experimental setup. (c) Schematic description of the noninterfering paths induced by two photons of parallel polarization and by two photon of orthogonal polarizations. (d) Schematic description of interfering paths induced by pairs of photons with parallel polarizations.

A simple approach to control the angular distribution would be to rotate the polarization of the excitation pulse from the x plane to the y plane at wavelengths larger than a specific wavelength [as shown schematically in the inset of Fig. 2(a)]. For such a pulse shape, there are always only two possible paths: one with two photons with parallel polarizations, and one by two photons with orthogonal polarizations. Since these two paths reach orthogonal final states, they do not interfere [see Fig. 1(c)]. Figure 2(a) presents the measured signal as function of the polarization step position. It shows that maximum population is achieved when the step is located at the central wavelength, so that each half-spectrum is orthogonally polarized. The transition from $|g,F,M\rangle$ to different $|f,F'',M''\rangle$ states is dictated by the selection rules described in Eq. (2). There are several limiting cases; when the step position is located at the edge of the pulse spectrum, the pulse is polarized along the $\hat{x}$ direction, therefore only the $|f,F'',M\rangle$ state is occupied. When the step is located at the center of the transition, only photon pairs of orthogonal polarization contribute to the transition, and only $|f,F'',M\pm1\rangle$ states are populated. Finally, when the entire spectrum is polarized along the $\hat{y}$ direction only $|f,F'',(M,M\pm2)\rangle$ are populated, where the total population is equal to the one induced by the $\hat{x}$

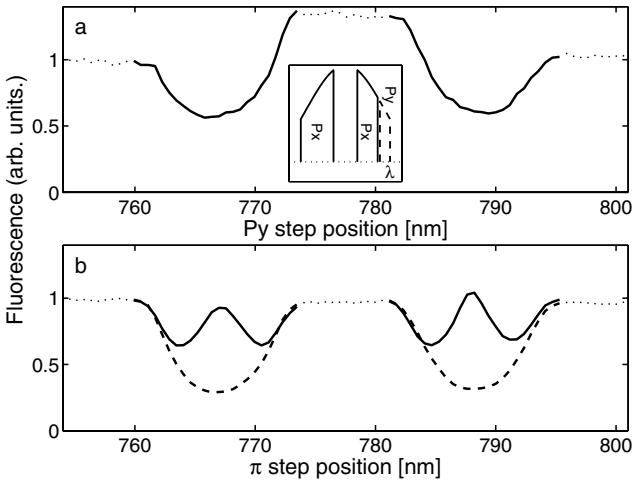

FIG. 2. TPA measurement for polarization and phase spectral manipulations. The TPA is measured for: (a) polarization-only filter as a function of the polarization step position (solid line). (b) phase-only filter as a function of a π step position (dashed line), and with a constant polarization step located at 788 nm (solid line). Inset: Schematic drawing of the spectral polarization of the electric field.

polarization. The measured signal is dictated by the ratio between the matrix elements of the different transitions corresponding to different values of ΔM [14].

Phase only control has been used previously to control the yield of TPA by inducing destructive interference between photon pairs populating the same final state [7]. A π phase step acts as a dimmer switch; by shifting its position in the spectrum, we can turn the transition rate on and off. When the entire spectrum of the input pulse is linearly polarized, all photon pairs interfere in reaching the same final state, as shown in the dashed line in Fig. 2(b). As discussed above, a polarization step induces a transition to two orthogonal final states. By combining a phase step with a polarization step, we can similarly tune the strength of each of the transitions separately without affecting the orthogonal one. Note that the interference here is between contributions of photon pairs which have similar polarizations but are comprised of photons with different energies. The solid line shows the response when a constant polarization step is located at $\omega_P = 788$ nm, and a phase step sweeps across the spectrum. Two distinct spectral regions, symmetric around $\lambda = 778$ nm, are induced, each contributing to a different ΔM transition. As is evident, the signal has four minima related to minimal population of each of the two states. The minima at $\lambda = 764, 792$ nm appear when the "dimmer switch" is applied to the $|f, F'', M \pm 1\rangle$ final states, induced by photon pairs of orthogonal polarizations. Similarly, the minima at $\lambda = 771, 785$ nm appear when the dimmer switch is applied to the $|f, F'', M\rangle$ final state, induced by photon pairs of parallel polarization. The signal reconstructs when the phase step location, w_{ph}, is equal to ω_P or to $\omega_{fg} - \omega_P$. In this case we introduce a constant phase between photon pairs that induce transitions to orthogonal final states. Indeed, the TPA signal was found to be independent of the relative phase of the E_xE_x and E_xE_y terms [see Fig. 1(c)].

The above scheme can be generalized by sweeping both the polarization and the phase steps to generate the control map shown in Fig. 3. The 2D image describes the measured signal as a function of the polarization step position (along the vertical direction) and as a function of a π phase step position (along the horizontal direction). The perimeter of the image is equivalent to phase only and polarization only control curves, respectively, as presented in Fig. 2. Three distinct spectral regions are observed. In each region the position of the π step controls the population of specific $|f, F'', M''\rangle$ states, where the orthogonal state population remains unchanged. The different regions are bounded by lines at 45° of the reconstructed population which are related to the maxima appearing in Fig. 2(b).

A different control scheme involves the interference between paths reaching the same final state but through intermediate states with different angular momentum [as shown in Fig. 1(d)]. In phase-only control, this interference pattern can be used for energy dependent spectroscopy of the intermediate states (CARS,TPA). This idea can now be extended either to provide spectroscopic information on degenerate intermediate states with different angular momenta, or to enhance the controllability of the final state. Consider, for example, the population at $|f, F'', M\rangle$ states ($\Delta M = 0$). As shown in Fig. 1(d), this is

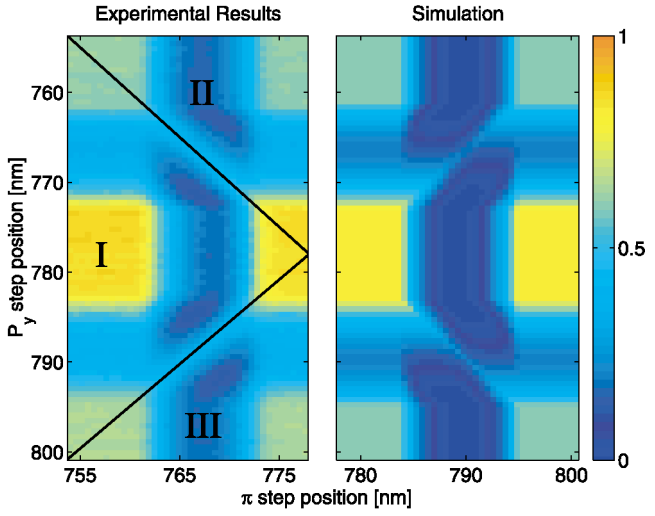

FIG. 3 (color). TPA measurement (left panel) and calculated result (right panel) as a function of the polarization step position (along the vertical direction) and the π phase step position (along the horizontal direction). In region I we control the transitions induced by photon pairs with orthogonal polarizations, corresponding to $|f, F'', M \pm 1\rangle$ states. In regions II and III we control the transitions induced by photon pairs with parallel polarization, corresponding to $|f, F'', M, M \pm 2\rangle$ states. The measurement and calculated images are inverted, due to the symmetry about half of the two photon transition frequency.

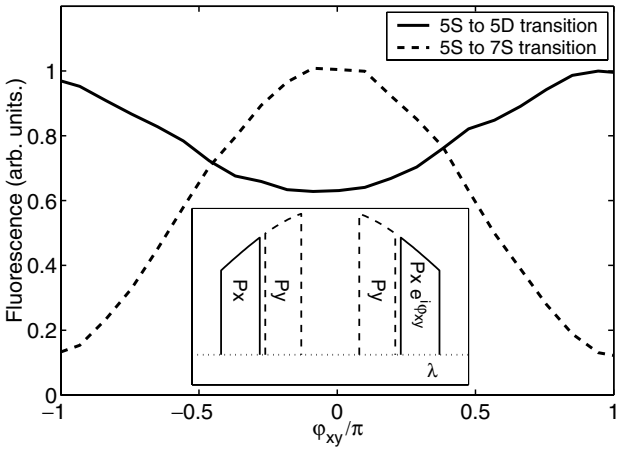

FIG. 4. TPA population measurement for a constant spectral polarization function and a variable phase step, setting a relative phase between the E_xE_x and the E_yE_y terms. The signal is measured as a function of the relative phase for the $5S \rightarrow 5D$ transition (solid line) and for the $5S \rightarrow 7S$ transition (dashed line). Inset: Schematic drawing of the spectral polarization and phase of the electric field used in the experiment.

determined by the interference between photon pairs with parallel polarizations. Controlling the relative phase between the two different angular momentum paths enables control of the $\Delta M = 0$ state population. If the final state is composed of a number of degenerate states with different complex matrix elements, selective excitation can be achieved in a manner similar to Shapiro's and Brumer's coherent control scheme for the selective excitation of photodissociation channels [2,12]. A particular channel can be maximized by setting the relative phase , φ_{xy}, between photon pairs of $\hat{x}$ and $\hat{y}$ polarizations to compensate for the phase differences, $\varphi = \arg(\mu^0_{nf}\mu^0_{gn}/\mu^{-1}_{nf}\mu^1_{gn})$, between paths leading to this channel.

In order to demonstrate this form of control, we rotated the polarization from the $\hat{x}$ axis to the $\hat{y}$ axis in a spectral band of 20 nm symmetrically around $(\omega_{fg}/2)$. An additional phase step was applied, which spectrally overlapped the long wavelength polarization step, to change the relative phase φ_{xy} between the E_xE_x and the E_yE_y components (see inset in Fig. 4). TPA in this case is induced only by photon pairs of parallel polarization, therefore according to Eq. (2) the possible final states are $|f, F'', (M, M \pm 2)\rangle$ [as shown in Fig. 1(d)]. TPA was measured for two different transitions, the $5S - 5D$ transition, as previously described, and the $5S - 7S$ transition. Figure 4 presents the measured signal as a function of the phase difference φ_{xy}. As is evident, TPA of the $5S - 5D$ transition is maximized for a relative phase of $\varphi_{xy} = \pi$, while the TPA of the $5S - 7S$ transition is maximized for $\varphi_{xy} = 0$. These different phases can be shown to relate to the different symmetry of the $5D$ and the $7S$ states. We note that while in atomic systems the relative phases of these two paths is either 0 or π, this is not necessarily true in molecular systems.

In this Letter we have established how the angular momentum distribution of the final state in a TPA process can be controlled by application of the phase-and-polarization shaping technique. These schemes utilize quantum interference to reveal both energy and angular momentum dependent spectroscopic information on either the intermediate or the final states. Previous coherent control schemes for selective excitation of degenerate levels required either the use of a different number of photons or at least one intermediate resonant state [2,15]. The scheme presented in this Letter enables control via a nonresonant transition induced by a single pulse. Angular distribution control induced by ultrashort pulses can be applied to control the *transient vector* properties of different processes such as the control of the evolution of wave packet angular momentum [4], molecular alignment, and the control of various photodissociation processes.

The authors wish to thank Moshe Shapiro, David Tannor, and Nir Davidson for fruitful discussions.

[1] D. J. Tannor and S. A. Rice, J. Chem. Phys. **83**, 5013 (1985).
[2] M. Shapiro and P. Brumer, J. Chem. Phys. **84**, 4103 (1986).
[3] R. S. Judson and H. Rabitz, Phys. Rev. Lett. **68**, 1500 (1992).
[4] T. C. Weinacht, J. Ahn, and P. H. Bucksbaum, Nature (London) **397**, 233 (1999).
[5] R. Bartels *et al.*, Nature (London) **406**, 164 (2000).
[6] A. Assion *et al.*, Science **282**, 919 (1998).
[7] D. Meshulach and Y. Silberberg, Nature (London) **396**, 239 (1998); Phys. Rev. A **60**, 1287 (1999).
[8] N. Dudovich *et al.*, Phys. Rev. Lett. **86**, 47 (2001); N. Dudovich, D. Oron, and Y. Silberberg, Phys. Rev. Lett. **88**, 123004 (2002).
[9] J. Degert *et al.*, Phys. Rev. Lett. **89**, 203003 (2002).
[10] B. Broers, L. D. Noordam, and H. B. van Linden van den Heuvell, Phys. Rev. A **46**, 2749 (1992); P. Balling, D. J. Maas, and L. D. Noordam, Phys. Rev. A **50**, 4276 (1994).
[11] T. Brixner and G. Gerber, Opt. Lett. **26**, 557 (2001); T. Brixner *et al.*, Appl. Phys. B **74**, S133 (2002).
[12] C. Asaro, P. Brumer, and M. Shapiro, Phys. Rev. Lett. **60**, 1634 (1988).
[13] J. R. Waldeck, M. Shapiro, and R. Bersohn, J. Chem. Phys. **99**, 5924 (1993).
[14] The measured contrast is dictated by the matrix elements of the three photon transition to level 6P and by position of the PMT.
[15] Z. Chen, P. Brumer, and M. Shapiro, Chem. Phys. Lett. **198**, 498 (1992).